

CONSTRUCTION OF A 4D WATER ICE CLOUD DATABASE FROM MARS EXPRESS / OMEGA OBSERVATIONS – DERIVATION OF THE DIURNAL MARTIAN CLOUD LIFE CYCLE

A. Szantai, *Laboratoire de Météorologie Dynamique, (CNRS/UPMC/IPSL), Paris, France (szantai@lmd.polytechnique.fr)*, **J. Audouard**, *Laboratoire Atmosphères, Milieux, Observations spatiales, (CNRS/UVSQ/IPSL), Guyancourt, France*, **F. Forget, J.-B. Madeleine, A. Pottier, E. Millour**, *Laboratoire de Météorologie Dynamique, (CNRS/UPMC/IPSL), Paris, France*, **B. Gondet, Y. Langevin, J.-P. Bibring**, *Institut d'Astrophysique Spatiale, (CNRS, Université Paris 11), Orsay, France*.

Introduction:

The purpose of this study is to obtain a better representation of Martian water ice clouds at global scale, in order to better understand the physical and dynamical processes taking place in the atmosphere (and on the surface). Up to now very few extensive studies based on satellite observations have described the cloud life cycle over several Martian years and over the day (Tamppari et al., 2003). Most recent satellites (MGS, Odyssey, MRO) are heliosynchronous and observe the planet only at specific local times (typically 2:00 – 3:00 a.m. and p.m. local time (LT)) over the largest part of their orbit. Mars Express, which carries the OMEGA spectro-imager can cover all periods of the day and thus can provide data useful for the determination of the cloud life cycle. It has retransmitted images over a long period, more than 6 Martian years (MY 26-32), and is still in operation.

Cloud extraction methodology:

Definition and calculation of the IceCloudIndex. The OMEGA spectro-imager provides images of the albedo of the Martian surface and atmosphere at different visible and near-IR wavelengths, between 0.3 and 5.1 μm . For a given pixel, the depth of a water absorption band or its slope between two close wavelengths indicates the presence and abundance of water ice clouds. This method was first applied on spectels in the 1.5 μm absorption band. But the slope of the absorption band at 3.2 μm enables a better detection of water ice clouds (Langevin et al., 2007). It has been applied on a small number of images and proved its efficiency (Madeleine et al., 2012).

In this study, we use the slope at 3.2 μm and define the original ice cloud index with the relation :

$$\text{ICIo} = I_{3.38\mu\text{m}} / I_{3.52\mu\text{m}}$$

where $I_{3.38\mu\text{m}}$ and $I_{3.52\mu\text{m}}$ are the albedos at the corresponding wavelengths close to the bottom, respectively close to the top of the absorption band.

We use preferably the normalized ice cloud index :

$$\text{ICI} = 1 - \text{ICIo}$$

A stronger absorption, produced by a thicker or denser water ice cloud, corresponds to an ICiO

closer to 0 and an ICI closer to 1, and the absence of cloud to an ICI value close to 0.

The images at 3.38 and 3.52 μm are extracted from all the OMEGA non-limb orbit segments, the corresponding ICI images are then calculated and each pixel undergoes a series of quality checks. Figure 1 shows an example of an ICI image, and the corresponding RGB image derived from the images at 3 visible wavelengths.

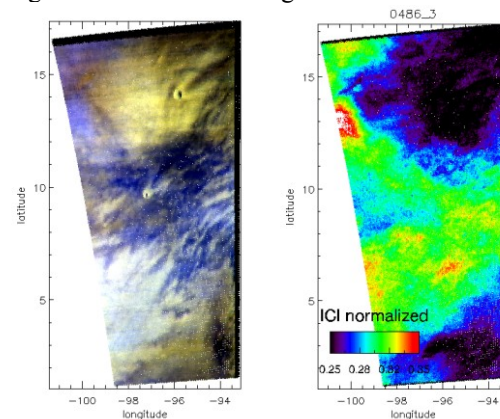


Figure 1: RGB OMEGA image at 3 visible wavelengths, with water ice clouds in bluish white and light purple (left) ; corresponding IceCloudIndex image (clouds from blue: 0.28 to red: 0.35) (right).

Construction of a 4-dimensional cloud database. In order to get a better knowledge of the Martian climate, and in particular its daily evolution over the Martian year, we define a regular grid :

1° longitude X 1° latitude X 5° solar longitude (Ls) X 1 h local time (LT)

and use it to construct a 4D water ice cloud database.

In practice we use the ICI values of all the valid (quality checked) pixels from all the orbit segments and bin them onto this grid, according to their spatio-temporal coordinates. Eventually the average IceCloudIndex, $\langle \text{ICI} \rangle$ is calculated for each 4D position (bin) where pixels were present.

This binning over pixels and orbits covering several Martian years is based on the assumption that the Martian climate does not change much between different years. This assumption is valid for most years and seasons (Smith, 2004), with one

notable exception, the periods of global dust storms. Only one such period has been observed by Mars Express during the processed period (2004-2015): the global dust storm of MY 28, $L_s = 261^\circ - 312^\circ$. Therefore the corresponding OMEGA images have been excluded from the 4D binning process.

Figure 2, top, shows an image of the $\langle ICI \rangle$, averaged over the northern spring period ($L_s = 45^\circ - 135^\circ$) and over daytime (7 – 17 h LT). The main cloud features (Aphelion Belt, Hellas Planitia, edges of the southern polar hood, northern hemisphere polar clouds...) are detected. Clouds are not detectable over the South Pole area, due to the polar night.

Although several thousands of Mars Express orbits have provided OMEGA data over more than 10 years, the spatio-temporal coverage on our high-resolution 4D grid is very small: only about 1 % of the grid-points have been covered by one or several orbits.

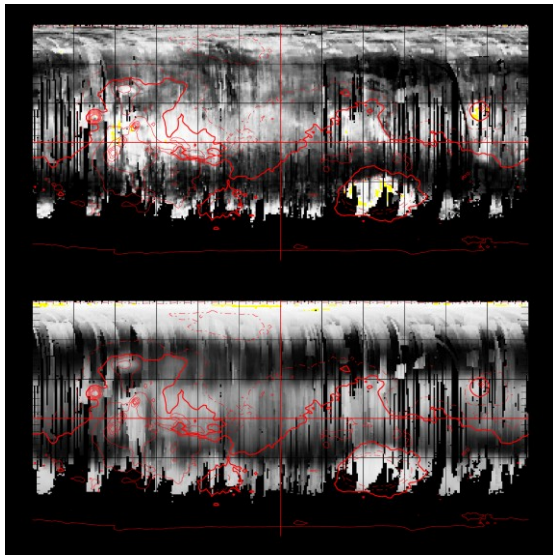


Figure 2: ICI image, averaged around the northern summer solstice ($L_s = 45^\circ - 135^\circ$) and over daytime (7 – 17 h LT) (top). WaterIceCol from the MCD, averaged at the same resolution and over the same period (bottom).

Comparison of TES optical depth with OMEGA Ice Cloud Index:

The optical depth of clouds and other atmospheric and surface products have been derived from spectra measured by the TES instrument onboard MGS (Smith, 2003). In this study, we compare the water ice optical depth τ_{ice} at $12.1 \mu m$, which has been mapped on a regular grid, to the average Ice Cloud Index $\langle ICI \rangle$ from OMEGA. The mapped TES τ_{ice} has the following characteristics:

- grid : 7.5° longitude x 3° latitude x 5° L_s .
- usable local time LT ~ 14 h in non-polar regions (determined by MGS's heliosynchronous orbit).

- covered period : one Martian year. In our case we use values from MY 24 hybrid (Mainly MY 24, completed by the beginning of MY 25 – before the global dust storm).

For this comparison, we have recalculated the average ice clouds index $\langle ICI \rangle$ over the same 3D grid at the same local time (14 h). Figure 3 shows an averaged map around the summer solstice period of both datasets : the location and relative thickness of cloudy (and cloudless) areas is quite similar. More frequent or thicker clouds can be observed in the Aphelion Belt, on the eastern part of Arabia Terra, around Elysium Mons, and to a lesser extent, on the northern edge of the Hellas basin. The relation between $\langle ICI \rangle$ and τ_{ice} is also reflected in the cross-correlation values : 0.61 for tropical-temperate latitudes ($|\text{latitude}| < 60^\circ N$) and 0.69 in the tropics ($|\text{latitude}| < 25^\circ N$).

A similar comparison of $\langle ICI \rangle$ data with corresponding TES τ_{ice} values from MY 26 gives similar qualitative results.

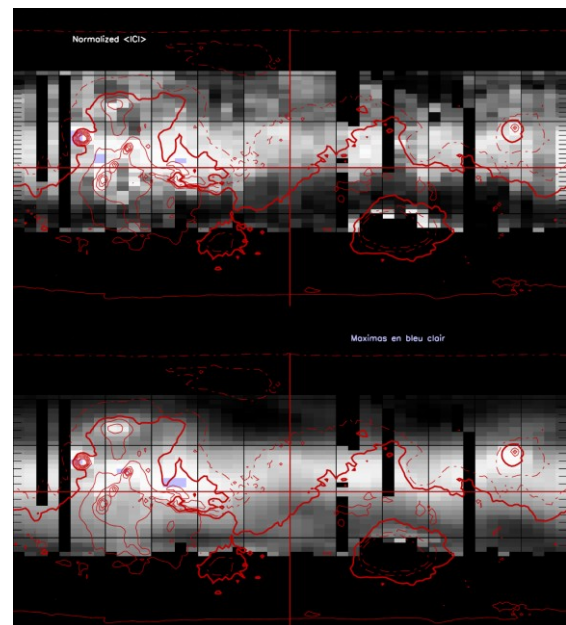


Figure 3 : ICI image (top) and TES τ_{ice} (bottom), averaged around the northern summer solstice ($L_s = 45^\circ - 135^\circ$) and over daytime (7 – 17 h LT), at the reduced spatial resolution.

Comparison of OMEGA averaged ICI with the water ice column from the MCD:

The general circulation model (GCM) developed at the LMD has been adapted to the planet Mars (Forget et al., 1999). Meteorological fields resulting from its simulations have been collected in the Mars Climate Database (MCD – Current version 5.2) (Millour et al., 2015). We compared the $\langle ICI \rangle$ derived from OMEGA spectral images to the integrated water ice column (WaterIceCol) extracted from the MCD and interpolated on the same

4D grid (1° longitude x 1° latitude x 5° Ls x 1 h local time).

Spatial comparison of datasets. Figure 2 shows the ICI from OMEGA and the WaterIceCol from the MCD averaged during daytime (7-17 h LT) around the summer solstice (Ls = 45-135°). Similar cloudy areas can be observed again, over the same areas as on the TES τ_{ice} images : Hellas Planitia, Aphelion Belt region, eastern Arabia Terra and Syrtis Major. Fewer outstanding cloudy areas are present on both corresponding datasets during northern winter (Ls = 225-315°) : the most noteworthy feature is the southern edge of the north polar hood (not shown).

Determination of the diurnal cloud life cycle. Due to the small percentage of ICI values on the 4D grid, we had to average values over a larger area, in practice over a specific climatic zone or a topographical feature (typically : around a volcano) covering several tens of degrees in longitude and latitude. Among 17 test areas, we selected two of them which show a good OMEGA data coverage and highlight the daily lifecycle over significant parts of the Martian year :

- The tropical region between the Tharsis volcano range and Elysium Mons (25°S – 25°N ; 90°W – 120°E).

- The Hellas Planitia region (55°S – 25°S ; 40°E – 105°E).

WaterIceCol values are available for all grid-points, but values corresponding to positions without ICI values can be masked out. The IceCloudIndex over these regions can then be directly compared to the WaterIceCol variable of the MCD.

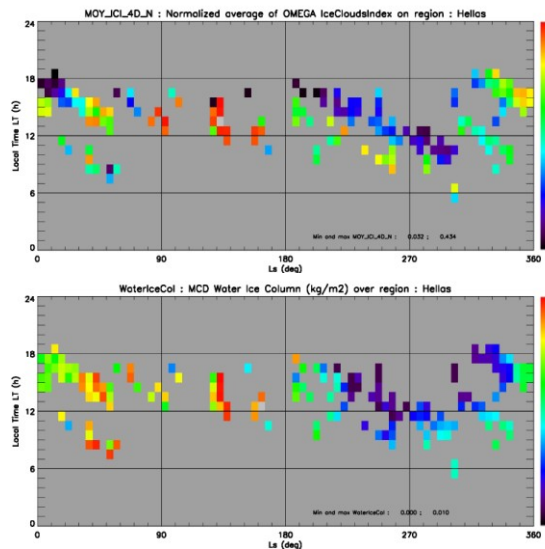


Figure 4 : diurnal cycle of the Ice Cloud Index (top) and Water Ice Column (bottom) over the Hellas Planitia area during one Martian year. Color range : from black, dark blue : lowest values ; to orange, red : highest values.

Figure 4 shows both variables over the Hellas Planitia area. The following evolutions can be observed :

- Clouds dissipate earlier and earlier before the southern summer solstice (between Ls = 180° and 270°). This trend can be explained by the decreasing influx of humidity from its main source, the North Polar Cap, and by the higher temperature resulting from increased insolation. After the solstice, this trend reverses.

- A relatively important cloudiness can be observed after the southern autumn equinox (around Ls = 45°) during a large part of the day, a larger/thicker cloud cover is present during the southern winter (around Ls = 135°), which can be related to the important release of water vapor from the North Polar Cap.

- A marked difference between both datasets is the absence of clouds at the end of the afternoon, shortly after the southern autumn equinox (Ls = 0°) on the ICI data only. If confirmed, insufficient available humidity could explain this phenomenon.

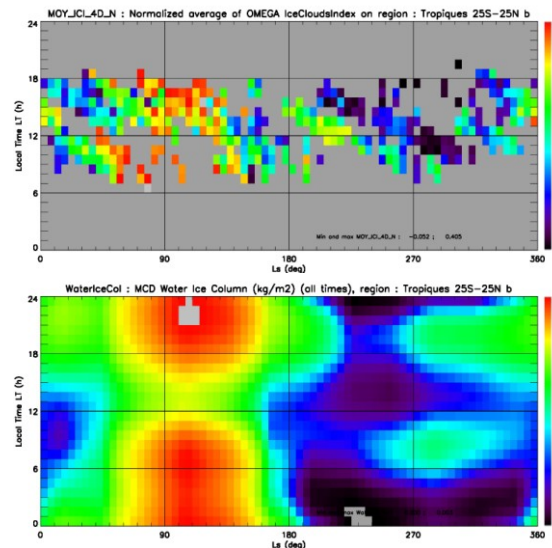


Figure 5 : diurnal cycle of the Ice Cloud Index (top) and Water Ice Column (bottom) over the tropical zone (-25°S – 25°N) during one Martian year. Color range : from black, dark blue : lowest values ; to orange, red : highest values.

The selection of a large climatic band between the tropics produces a more complete dataset for diurnal cycle comparisons. Figure 5 shows the ICI and the WaterIceCol variables, this time shown over all grid-points :

- The advance of cloud dissipation time before the northern winter solstice (between Ls = 200° and 270°) is similar to the one observed over the (non-overlapping) Hellas area, though less obvious, and can also be explained by the same mechanism, a decreasing influx of humidity from the north.

- Few clouds are present in the morning shortly after the northern spring equinox ($L_s \sim 30^\circ$).

- Around the summer solstice ($L_s \sim 90^\circ$), the important cloudiness is reduced at 12 h, before increasing again. With the help of complementary data from the MCD database, this evolution of the clouds and the minimal cloudiness can be explained by the propagation of a thermal tide which induces a temperature anomaly that controls the condensation-sublimation of the cloud ice (figure 6).

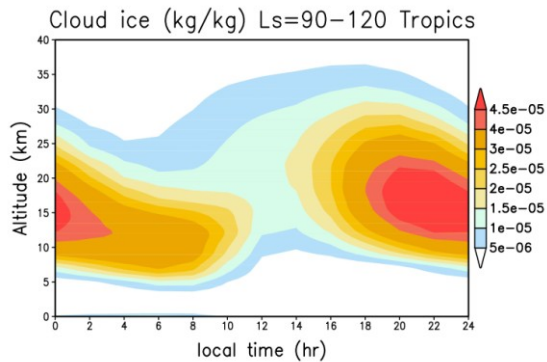


Figure 6 : MCD diurnal cloud ice density in the tropics at the beginning of summer ($L_s = 90^\circ - 120^\circ$).

Conclusion and prospects:

Our high-resolution 4D database, although sparsely populated, shows a cloud coverage similar to the optical thickness from TES (τ_{ice}) and to the water ice column calculated in the LMD Martian GCM. When integrated over a specific period and area, it can also show the daily evolution of the cloudiness. As an example, we found that the diurnal cycle in the tropics is characterized by important cloudiness in the morning, decreasing until noon, and increasing again in the afternoon ; this can be explained with model data by the action of a thermal tide.

This dataset will also be useful for complementary analyses, which have started at LMD in order to retrieve water ice cloud optical depth and particle size (see Olsen et al., this issue). It will also be useful for the validation of high-resolution model simulations of the Martian climate (Pottier et al., 2016).

Very recent and future missions of non-heliocentric satellites (MAVEN, Mangalayan, Exomars) may potentially provide complementary information and data on water ice clouds in a near future.

References:

F. Forget, F. Hourdin, R. Fournier, C. Hourdin, O. Talagrand, M. Collins, S.R. Lewis, P. Read and

J.P. Huot, 1999. Improved general circulation models of the Martian atmosphere from the surface to above 80 km. *J. Geophys. Res. (Planets)*, 104, 24155-24176. doi: 10.1029/1999JE001025 .

Y. Langevin, J.-P. Bibring, F. Montmessin, F. Forget, M. Vincendon, S. Douté, F. Poulet, and B. Gondet, 2007. Observations of the south seasonal cap of Mars during recession in 2004–2006 by the OMEGA visible/near-infrared imaging spectrometer on board Mars Express, *J. Geophys. Res.*, 112, E08S12, 32 pp. doi:10.1029/2006JE002841 .

J.-B. Madeleine, F. Forget, A. Spiga, M. J. Wolff, F. Montmessin, M. Vincendon, D. Jouglet, B. Gondet, J.-P. Bibring, Y. Langevin and B. Schmitt, 2012. Aphelion water-ice cloud mapping and property retrieval using the OMEGA imaging spectrometer onboard Mars Express. *J. Geophys. Res.*, 117, E00J07, 21 pp. doi: 10.1029/2011JE003940 .

E. Millour, F. Forget, A. Spiga, T. Navarro, J.-B. Madeleine, L. Montabone, A. Pottier, F. Lefevre, F. Montmessin, J.-Y. Chaufray, M.A. Lopez-Valverde, F. Gonzalez-Galindo, S.R. Lewis, P.L. Read, J.-P. Huot, M.-C. Desjean and the LMD development team, 2015. The Mars Climate Database (MCD version 5.2). *European Planetary Science Congress 2015*, 10, EPSC2015-438, October 2015.

K. S. Olsen, J.-B. Madeleine, L. Montabone, F. Forget, A. Szantai, J. Audouard, A. Geminalo, M. J. Wolff, 2017. The distribution of retrieved properties from water ice clouds in the Martian atmosphere using the OMEGA imaging spectrometer. *6th International Workshop on Mars Atmospheres : Modelling and observations, Granada, January 2017 (this issue)*, 4 pp.

A. Pottier, F. Forget, F. Montmessin, T. Navarro, A. Spiga, E. Millour, A. Szantai, J.-B. Madeleine, 2017. Unraveling the Martian water cycle with high-resolution global climate simulations. *Icarus* (submitted).

M. D. Smith, 2004. Interannual variability in TES atmospheric observations of Mars during 1999-2003. *Icarus*, 167, 148-165. doi: 10.1016/j.icarus.2003.09.010 .

L. K. Tamppari, R. W. Zurek and D. A. Paige, 2003. Viking-era diurnal water ice clouds. *J. Geophys. Res.*, 108, E7, 5073, 14 pp. doi: 10.1029/2002JE001911 .

